

# CONJUGATE HEAT TRANSFER PREDICTIONS FOR SUBCOOLED BOILING FLOW IN A HORIZONTAL CHANNEL USING A VOLUME-OF-FLUID FRAMEWORK

by

M. Langari, Z. Yang<sup>a</sup>, J. F. Dunne\*, S. Jafari,  
J-P Pirault, C. A. Long, and J. Thalackottore Jose

Department of Engineering and Design  
School of Engineering and Informatics  
University of Sussex, Falmer, Brighton, BN1 9QT, UK.

<sup>a</sup>Department of Mechanical Engineering and the Built Environment  
College of Engineering and Technology  
University of Derby, Markeaton Street, Derby DE22 3AW, UK

\* Corresponding author: E-mail: [j.f.dunne@sussex.ac.uk](mailto:j.f.dunne@sussex.ac.uk)

## **SUMMARY**

The accuracy of CFD-based heat transfer predictions have been examined of relevance to liquid cooling of IC engines at high engine loads where some nucleate boiling occurs. Predictions based on: i) the Reynolds Averaged Navier-Stokes (RANS) solution, and ii) Large Eddy Simulation (LES), have been generated. The purpose of these simulations is to establish the role of turbulence modelling on the accuracy and efficiency of heat transfer predictions for engine-like thermal conditions where published experimental data is available. A multi-phase mixture modelling approach, with a Volume-of-Fluid interface-capturing method, has been employed. To predict heat transfer in the boiling regime, the empirical boiling correlation of Rohsenow is used for both RANS and LES. The rate of vapour-mass generation at the wall surface is determined from the heat flux associated with the evaporation phase change. Predictions via CFD are compared with published experimental data showing that LES gives only slightly more accurate temperature predictions compared to RANS but at substantially higher computational cost.

Keywords: Flow boiling; IC engines; CFD; Large Eddy Simulation; Reynolds Averaged Navier-Stokes.

8 main-section pages (double spaced) 25 references Figures 1 – 8 No Appendices

## 1. INTRODUCTION

Predicting the heat transfer levels that occur in nucleate boiling is important for many engineering applications such as the cooling of micro-electronic devices and nuclear reactors [1]–[3]. This is of increasing importance for highly-boosted IC engines which, at full load, relies heavily on a degree of nucleate boiling to operate at the limits of conventional liquid cooling systems [4]-[6].

Despite extensive research [7]–[11], the mechanism of nucleate boiling heat transfer is still not fully understood. As a result, mechanistic models, based on bubble formation and the bubble departure phenomenon, are not yet able to predict nucleate boiling heat transfer. To provide a solution to this difficulty, empirical correlations are generally used in practical situations [8][12] particularly in automotive applications [13]-[17].

Appropriate thermal boundary layer and vapour formation modelling by contrast, is known to play a significant role in accurate predictions of heat transfer in the boiling regime [18][19]. Shala [19] used a 'mixture' two-phase model with a mechanistic nucleate boiling model to predict the wall heat flux and its partitioning into separate heat transfer mechanisms (i.e. single-phase convection, wall quenching, and evaporation). The results agree reasonably well with experimental data for both a horizontal channel flow, and flow in a vertical annulus, but significant under-prediction of heat flux occurs at higher velocities in both the convective and boiling regions. This shortcoming was associated with the turbulence model and the wall function used. Elsewhere Yun *et al.* [20] used the  $k$ - $\epsilon$  model with a special logarithmic velocity wall function for both liquid and vapour phases, and a mechanistic bubble-size model in their two-fluid Eulerian CFD simulation for subcooled boiling flow prediction. Although improved prediction of phase velocities were achieved with this wall function, they highlighted the need for improved turbulence models for two-phase boiling flows. And motivated by the possibility that an LES approach to turbulence modelling may provide better thermal predictions in flow boiling situations, Deen *et al.* [21] investigated the

performance of Eulerian-Eulerian RANS and LES approaches for a liquid-gas flow (i.e. with no heat transfer). They showed that LES gave better agreement with experimental data than the RANS  $k-\varepsilon$  model simulations.

Despite the past decade seeing massive growth in CFD modelling with complex geometries, accurate prediction of pointwise heat transfer between a solid surface and a two-phase flow, still remains a major challenge. In this paper, a two-phase LES approach for heat transfer prediction in flow boiling conditions is examined. This is accomplished by comparing RANS and LES simulations on a horizontal channel flow with heating from the lower surface. Simulations are undertaken by means of the finite-volume CFD solver STAR\_CCM+.

## 2. THE NUMERICAL MODELLING FRAMEWORK

Liquid and vapour flow are simulated using the VOF Multiphase modelling approach within the Eulerian framework (originally proposed in [22]). One set of governing equations are solved for the mixture flow with shared velocity, pressure, and temperature fields, assumed for the two phases. An additional phase fraction equation is used to calculate the spatial phase concentrations within the domain. The equations are solved for an equivalent fluid whose physical properties are calculated as functions of the physical properties of its constituent phases and their volume fractions. The governing equations and the conservation equation that describe the transport of volume fraction of phase are fairly standard, and hence will not be presented here, [which can be found in \[23\]](#)

The convective part of the heat transfer is computed from [\[23\]](#):

$$q_c = h_c(T_w - T_c) \quad (1)$$

and

$$h_c = \frac{\rho_{f|y_c} c_{p.f|y_c} u_\tau}{T^+ y^+|_{y_c}} \quad (2)$$

where  $q_c$  is the convective heat flux,  $h_c$  is the convective heat transfer coefficient,  $T_w$  is the wall temperature,  $T_c$  is the local near-wall cell temperature,  $u_\tau$  is the friction velocity,  $T^+$  is the dimensionless temperature,  $y_c$  is the normal distance of the near wall cell, and  $y^+$  is the dimensionless wall distance  $u_\tau y_c / \nu_f$  and  $\nu_f$  is kinematic viscosity of the fluid.

A grid independency test has been undertaken for RANS simulations where a final grid of 434300 cells is chosen with particular attention paid to the discretization of near-wall regions. Boundary layers are resolved by appropriate near-wall prism layers, with the near-wall thickness resolution in the region  $2.0 < y^+ < 25$ . Three turbulence models: the realisable  $k-\epsilon$  mode, the SST  $k-\omega$  mode, and the  $k-\epsilon$  v2-f model are employed with a hybrid wall function called the: 'All  $y^+$ ' wall approach in STAR\_CCM+ [23] for near-wall turbulence quantities. In the RANS simulations, the mesh is not fine enough to resolve the interface between the liquid and the vapour phase. The interface however is captured directly in the LES simulations as a much finer mesh is used.

LES computations have been achieved on a  $950 \times 40 \times 60$  structured grid (i.e.  $\sim 2280000$  cells) with a refined near-wall grid to ensure the nearest wall cell  $y^+ < 1$ . Wall Adapting Local Eddy (WALE) Subgrid Scale model is employed [24]. The LES inlet flow is generated by mapping instantaneous velocity and turbulent field data tables extracted from a precursor channel flow simulation. The temporal and spatial fidelity of LES is ensured by applying bounded-central-differencing and second-order temporal discretization. The time-step size is chosen to maintain a convective Courant Number smaller than 1. For each thermal load, simulations are continued until enough samples have been collected to obtain the mean wall temperature.

## 2.1 Phase-change model

The phase change model used, accounts for the onset of boiling through a number of sub-models. The heat transfer at the wall-to-fluid boundary is used to calculate the phase change mass transfer rate. The vapour-phase temperature is assumed constant at the saturation

temperature  $T_{sat}$ , and the liquid temperature  $T_f$  is approximated by the mixture temperature  $T$ . The total heat interchange between the liquid and vapour-phases is then used to specify the mass transfer between phases i.e.:

$$\dot{m}_{ec} = \frac{C_{HTC \times Area}(T - T_{sat})}{h_{fg}} \quad (3)$$

where  $C_{HTC \times Area}$  is the product of the heat transfer coefficient between the vapour bubbles and adjacent liquid, with the contact area separating the two phases, where  $h_{fg}$  is the phase change enthalpy. Boiling occurs at the liquid-solid surface interface where the wall temperature is higher than  $T_{sat}$ . The surface heat flux  $q_{bw}$ , as a result of boiling, is calculated using the empirical correlation of Rohsenow [8] given as follows:

$$q_{bw} = \mu_f h_{fg} \sqrt{\frac{g(\rho_f - \rho_g)}{\sigma}} \left( \frac{c_{p,f}(T_w - T_{sat})}{C_{qw} h_{fg} Pr_f^{1.7}} \right)^{3.03} \quad (4)$$

where  $\mu_f$ ,  $c_{p,f}$ ,  $Pr_f$  are respectively the dynamic viscosity, the specific heat, and the Prandtl Number of the liquid phase;  $g$  is the gravitational acceleration,  $\rho_g$  is the density of the vapour-phase,  $\sigma$  is the surface tension at the liquid-vapour interface, and  $T_w$  is the wall temperature.

### 3. MODEL PARAMETERS AND EXPERIMENTAL VERIFICATION GEOMETRY

The geometry and flow conditions of an experimental study [25] are used for the current RANS and LES simulations including conjugate heat transfer (CHT). The value of the empirical coefficient  $C_{qw}$  in equation (4), is a function of the particular liquid-surface combination. A chosen value of  $C_{qw} = 0.0029$  is considered to represent the water-OAT (Organic Acid Technology) coolant mixture (at 90°C, the inlet flow temperature used in the present study, the properties of this mixture are:  $\rho = 1038 \text{ kg/m}^3$ ,  $\mu = 0.00085 \text{ kg/ms}$ ,  $k = 0.424 \text{ W/mK}$  and  $C_p = 3620 \text{ J/kgK}$ ) and the aluminium alloy used in the rig from which experimental data were obtained in [14] [25].

### 3.2 Geometry and boundary conditions

Figure 1 shows the geometry of the 3D CFD/CHT model. Figure 2 shows a view of the grid for the fluid (top) and solid domains. The fluid is a mixture of water-OAT coolant with 50% volumetric ratios and with the physical properties as defined in [14] [25] where a set of test conditions are available at different pressures, inlet velocities, and temperatures.

Simulations have been obtained at the highest boiling potential condition i.e. the lowest coolant velocity of 0.25 m/s with an inlet temperature of 90 °C, a coolant pressure of 1.0 bar (absolute), and a corresponding saturation temperature of 108 °C. The RANS simulation inlet boundary is defined with a uniform inlet velocity profile. The inlet turbulence intensity has been assumed to be 5%, typical for low Re number pipe-flows (where  $Re=5800$  in the current study based on channel height and inlet condition). A convective outflow boundary condition is applied at the outlet. The heating power applied to the heating section (to match the experimental conditions) gives heat fluxes in the range 83 - 1300 kW/m<sup>2</sup>.

### 4. RESULTS

Figure 3 shows the predicted wall temperatures compared with the experimental data from [25] at different heat flux levels. It can be seen that the temperature predictions obtained by different turbulence models of the RANS approach compare very well with the experimental data, where the maximum difference is smaller than 3 °C except for the predictions obtained by the v2-f model at higher thermal loads. The LES predictions are a little closer to the experimental data, especially at the heat flux around 271 kW/m<sup>2</sup> where there is almost perfect agreement between the LES prediction and the experimental data. At lowest thermal loads the measured wall temperature of 107.4 °C is just below the saturation temperature of the liquid  $T_{sat}$  at 108 °C. For this case, the heat transfer is essentially the result of pure convection (no boiling contribution) whereas the predicted wall temperature of 109.6 °C obtained by both RANS and LES is slightly above the saturation temperature, which means that the boiling model (eq. 4) is activated in the prediction to work out the heat transfer

contribution due to boiling . This can be confirmed by Figure 4 which shows contours of the predicted vapour volume fraction obtained by LES and the realizable k-e model at the lowest heat flux, where it can be clearly seen that the predicted vapour volume fraction is not zero.

Although the LES simulations provide much better predictions of the turbulent flow field, in the present study, the complex process involved in the subcooled nucleate boiling flow, such as bubble nucleation, growth, detachment, coalescence and collapse, cannot be directly captured by LES. Therefore sub-models for boiling using empirical correlations have been employed in both the LES and RANS. As a consequence, the LES predictions of wall temperature show only marginal improvement over the RANS predictions as the temperature prediction depends strongly on the boiling sub-models. Nevertheless LES predictions can provide more information such as the instantaneous wall surface temperature distribution as shown in Figure 5. Another distinguishing feature that can be observed, is the instantaneous temperature distribution is very different from uniform in the span-wise direction - there are a few hot spots scattered in the downstream region. This may have serious implications for real engineering application as the averaged wall surface temperature could be well below a critical value whereas the instantaneous value might well not be. This kind of information can only be obtained from LES predictions.

It is evident from the current study that, in terms of the averaged wall temperature prediction, it is not essential to resolve the interface between the liquid and the vapour phase because the RANS predictions (without resolving the interface) are very close to the LES predictions (resolving the interface). Figure 6 shows that a clear interface can be seen in the LES prediction but not in the RANS prediction.

With regard to the v2-f model, the wall temperature is over-predicted at higher thermal loads. This may stem from the fact that boiling is under-predicted so that less heat transfer contribution from boiling, leading to slightly less total heat transfer predictions compared with other turbulence models. This results in slightly higher surface temperature. Figure 7 shows

the predicted vapour volume fraction obtained by different turbulence models at the highest thermal loads of  $1300 \text{ kW/m}^2$ . It can be seen that the vapour volume fraction obtained by the v2-f model is slightly lower than the predictions obtained by the other two turbulence models.

Figure 8 shows contours of the predicted turbulent intensity obtained by the realizable k-e model. Predictions by other turbulence models are actually very similar. It is evident that turbulence is mainly generated in the heated surface area as a result of heat addition and boiling.

## **5. CONCLUSIONS**

Numerical simulations have been undertaken for conjugate heat transfer predictions in thermal and flow conditions representative of coolant flow within IC engine cooling jackets. A multiphase mixture modelling approach with a Volume-of-Fluid interface capturing method has been employed for two phase flow combined with empirical correlations to predict heat transfer and phase change in the boiling regime. Both LES and RANS approaches have been employed in the study. The performance of LES, and a number of different turbulence models in RANS, are assessed by comparing the predicted wall temperatures with published experimental data. The main findings are:

- The predicted wall temperatures obtained by both the LES and RANS approaches are in good agreement with measured data, apart from the predictions using the v2-f model at high values of heat flux. This suggests that the multiphase mixture modelling approach, combined with the empirical correlations for boiling, employed in the present study, is an appropriate choice for simulating such flows.
- Compared to the RANS models, LES predictions of the wall temperature are only marginally closer to the experimental data. This stems from the fact that the same boiling sub-models are used in both the LES and RANS approaches. For sub-cooled nucleate

boiling flow conditions (as in the present study i.e. without flow separation and swirl), this finding suggests that it may not be advantageous to employ LES as the computational cost is significantly higher.

- It is not essential to resolve the interface between the liquid and the vapour phases. This is because the RANS predictions (without resolving interface) are very close to the LES predictions where the interface is resolved.
- Since Reynolds number in the current study is quite low, turbulence is mainly generated in the heated surface region as a consequence of heat addition and the action of boiling. This may be another reason for the relatively good agreement between RANS and LES predictions. However, this may not be the case for higher Reynolds number, where further study is needed.

## **Acknowledgments**

The authors wish to acknowledge funding support for this project from the EPSRC under Contract Number: EP/M005755/1. The technical support is also acknowledged of colleagues at Ford Dunton UK and Dearborn USA, Denso Italy, and the Ricardo Technical Centre Shoreham, UK.

## References

- [1] Kandlikar, S. G., 2002, "Fundamental issues related to flow boiling in minichannels and microchannels," *Exp. Therm. Fluid Sci.*, 26, pp. 389–407.
- [2] Mesquita, A. Z., and Rodrigues, R. R., 2013, "Detection of the Departure from Nucleate Boiling in Nuclear Fuel Rod Simulators," *Int. J. Nucl. Energy*, Volume 2013, Article ID 950129, 7 pages.
- [3] Suzuki, K., and Kawamura, H., 2004, "Microgravity experiments on boiling and applications: Research activity of advanced high heat flux cooling technology for electronic devices in Japan," in *Annals of the New York Academy of Sciences*, 1027, pp. 182–195.
- [4] Torregrosa, A. J., Broatch, A., Olmeda, P., and Cornejo, O., 2014, "Experiments on subcooled flow boiling in I.C. engine-like conditions at low flow velocities," *Exp. Therm. Fluid Sci.*, 52, pp. 347–354.
- [5] Robinson, K., Campbell, N. A. F., Hawley, J. G., and Tilley, D. G., 1999, "A Review of Precision Engine Cooling," SAE Tech. Pap. no.: 1999-01–0578.
- [6] Ap, N., and Tarquis, M., 2005, "Innovative Engine Cooling Systems Comparison," SAE Tech, Pap. no.: 2005-01–1378.
- [7] Sanna, A., Hutter, C., Kenning, D. B. R., Karayiannis, T. G., Sefiane, K., and Nelson, R. A., 2014, "Numerical investigation of nucleate boiling heat transfer on thin substrates," *Int. J. Heat Mass Transf.*, 76, pp. 45–64.
- [8] Rohsenow, W. M., 1952, "A Method of Correlating Heat Transfer Data for Surface Boiling of Liquids," *Trans. ASME*, 74, pp. 969–976.
- [9] Le Martelot, S., Saurel, R., and Nkonga, B. 2014, "Towards the direct numerical simulation of nucleate boiling flows," *Int. J. Multiph. Flow*, 66, pp. 62–78.
- [10] Mohanty, R. L., and Das, M. K., 2017, "A critical review on bubble dynamics parameters influencing boiling heat transfer," *Renew. Sustain. Energy Rev.*, 78, pp. 466–494.
- [11] Sun, T., Li, W., and Yang, S., 2013, "Numerical simulation of bubble growth and departure during flow boiling period by lattice Boltzmann method," *Int. J. Heat Fluid Flow*, 44, pp. 120–129.
- [12] Chen, J. C., 1966, "Correlation for boiling heat transfer to saturated fluids in convective flow," *Ind. Eng. Chem. Process Des. Dev.*, 5(3), pp. 322–329.
- [13] Steiner, H., Brenn, G., Ramstorfer, F., and Breitschadel, B., 2011, "Increased Cooling Power with Nucleate Boiling Flow in Automotive Engine Applications," in *New Trends and Developments in Automotive System Engineering*, InTech.
- [14] Robinson, K., Hawley, J. G., and Campbell, N. A. F., 2003, "Experimental and modelling aspects of flow boiling heat transfer for application to internal combustion engines," *Proc. Inst. Mech. Eng. Part D J. Automob. Eng.*, 217(10), pp. 877–889.
- [15] Cardone, M., Senatore, A., Buono, D., Polcino, M., De Angelis, G., and Gaudino, P., 2008, "A Model for Application of Chen's Boiling Correlation to a Standard Engine Cooling System," SAE Tech. Pap. no.: 2008–01–1817.

- [16] Fontanesi, S., and Giacomini, M., 2013, "Multiphase CFD-CHT optimization of the cooling jacket and FEM analysis of the engine head of a V6 diesel engine," *Appl. Therm. Eng.*, 2(2), pp. 293–303.
- [17] Carpentiero, D., Fontanesi, S., Gagliardi, V., Malaguti, S., Margini, S., Giacomini, M., Strozzi, A., Arnone, L., Bonanni, M., and Franceschini, D., 2007, "Thermo-mechanical analysis of an engine head by means of integrated CFD and FEM," *SAE Tech. Pap.* no.: 2007–24–0067.
- [18] Fontanesi, S., Carpentiero, D., Malaguti, S., Giacomini, M., Margini, S., and Arnone, L., 2008, "A New Decoupled CFD and FEM Methodology for the Fatigue Strength Assessment of an Engine Head," *SAE Tech. Pap.* no.: 2008–01–0972.
- [19] Shala, M., 2012, "Simulation of nucleate boiling flow using a multiphase mixture modelling approach," *IMA J. Appl. Math.*, 77(1), pp. 47–58.
- [20] Yun, B.-J., Splawski, A., Lo, S., and Song, C.-H., 2012, "Prediction of a subcooled boiling flow with advanced two-phase flow models," *Nucl. Eng. Des.*, vol. 253, pp. 351–359.
- [21] Deen, N. G., Solberg, T., and Hjertager, B. H., 2001, "Large eddy simulation of the Gas–Liquid flow in a square cross-sectioned bubble column," *Chem. Eng. Sci.*, 56(21–22), pp. 6341–6349.
- [22] Hirt C.W., and Nichols, B.D., 1981, "Volume of fluid (VOF) method for the dynamics of free boundaries". *Journal of Computational Physics*, 39 (1), pp. 201–225.
- [23] *STAR-CCM+ User Guide*, Version 11. CD-adapco, 2016.
- [24] Nicoud, F., and Ducros, F., 1999, "Subgrid-scale stress modelling based on the square of the velocity gradient tensor," *Flow, Turbul. Combust.*, 62(3), pp. 183–200.
- [25] Robinson, K., 2001, "IC engine cooling heat transfer studies," PhD thesis, University of Bath, UK.

## FIGURE CAPTIONS

Figure 1. Simulated channel geometry and heating block, dimensions in mm.

Figure 2. A section of the fluid/solid domain grid.

Figure 3. Predicted wall temperatures against experimental data [20].

Figure 4. Predicted vapour volume fraction at the lowest heat flux of 83 kW/m<sup>2</sup>.

Figure 5. A snapshot of wall surface temperature by LES at heat flux of 721 kW/m<sup>2</sup>.

Figure 6. Predicted vapour volume fraction at heat flux of 721 kW/m<sup>2</sup>.

Figure 7. Predicted vapour volume fractions by different turbulence models at heat flux of 1300 kW/m<sup>2</sup>.

Figure 8. Predicted turbulent intensity by realizable k-e turbulence model at heat flux of 721 kW/m<sup>2</sup>.

## LIST OF FIGURES

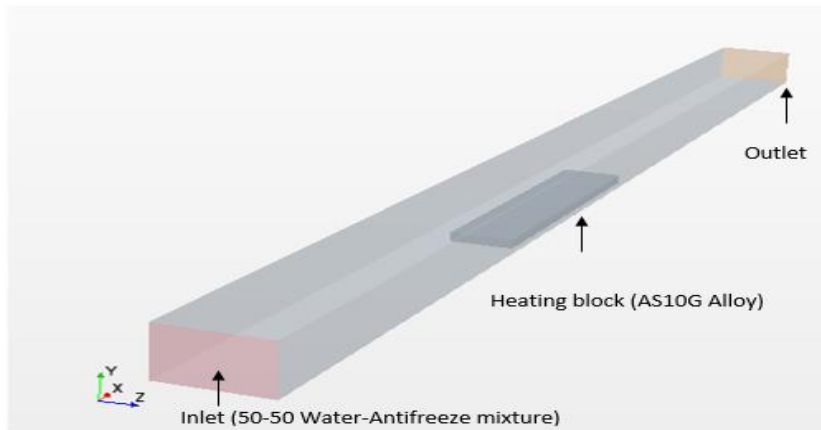
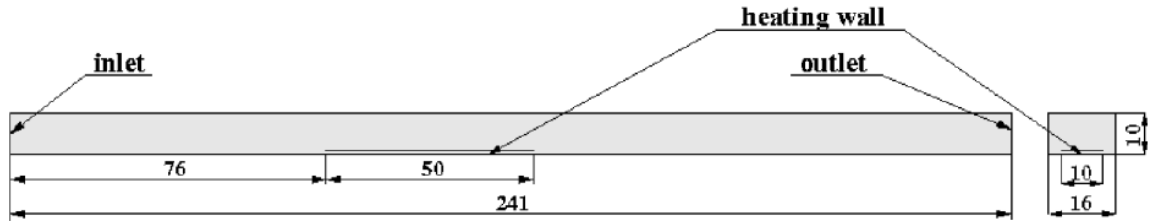


Figure 1. Simulated channel geometry and heating block, dimensions in mm.

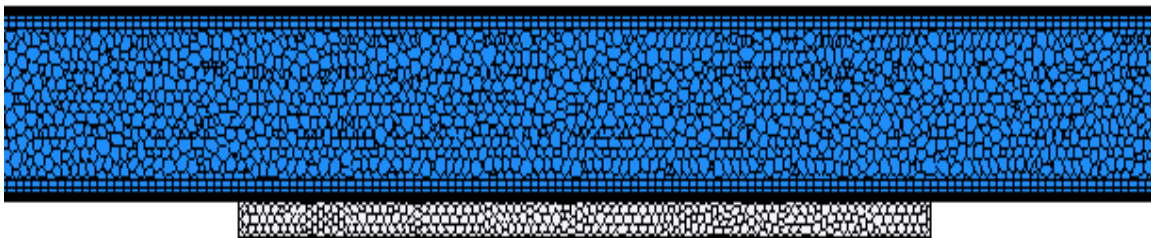


Figure 2. A section of the fluid/solid domain grid.

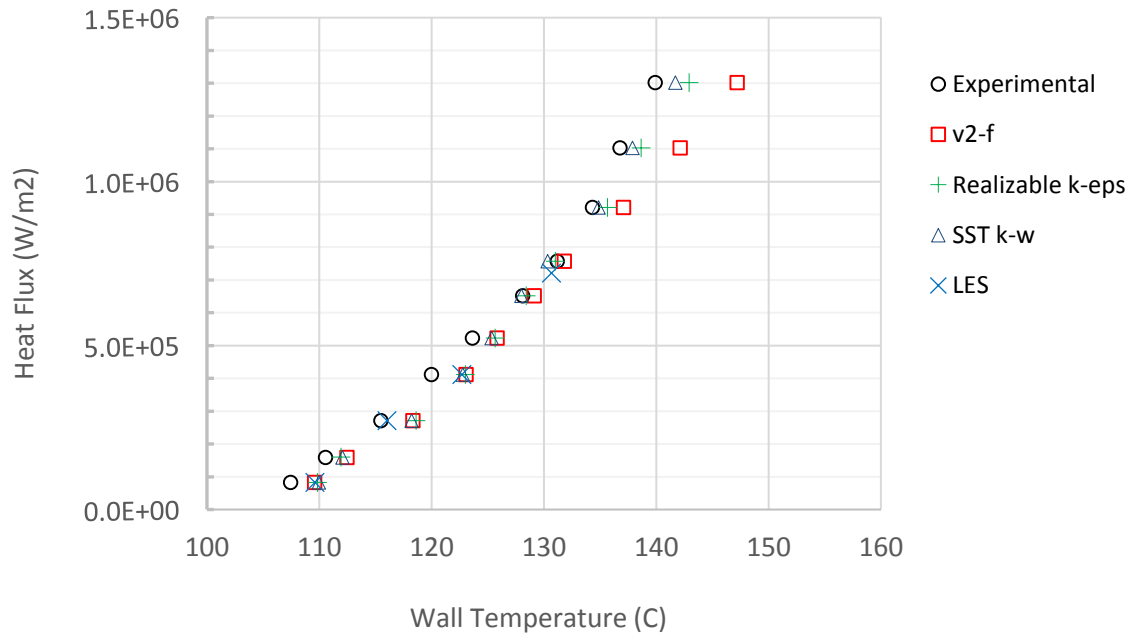


Figure 3. Predicted wall temperatures against experimental data [25].

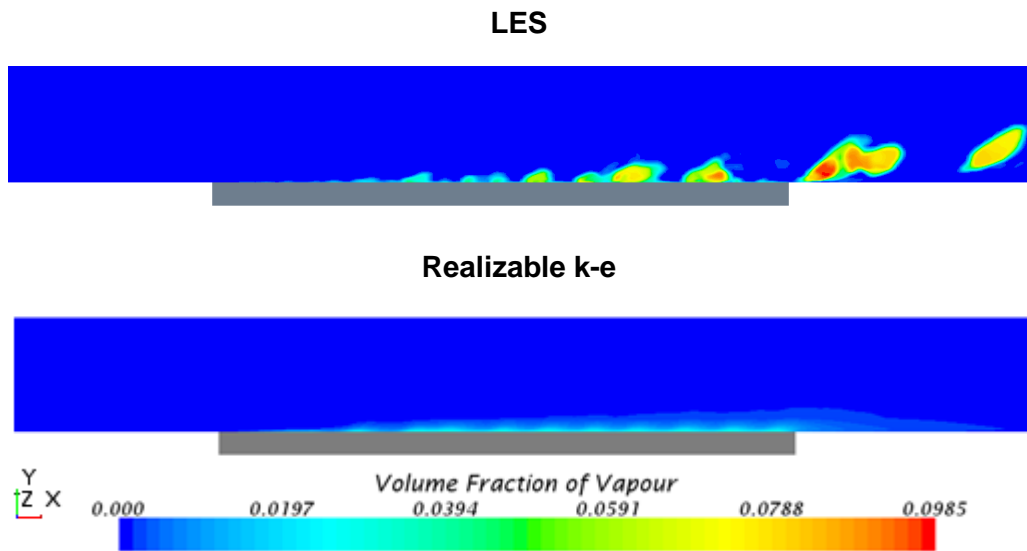


Figure 4. Predicted vapour volume fraction at the lowest heat flux of 83 kW/m<sup>2</sup>.

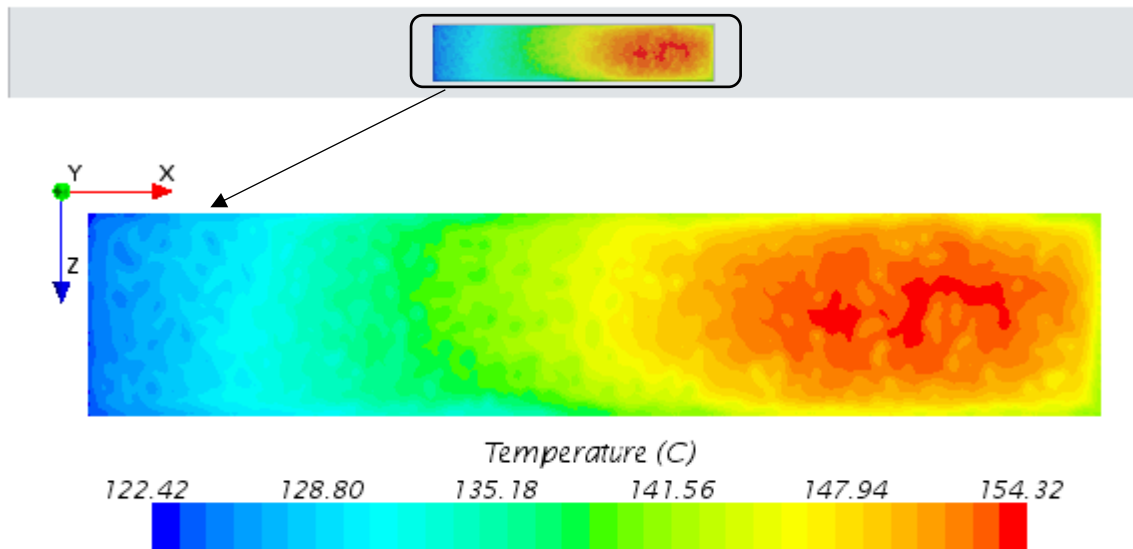


Figure 5. A snapshot of wall surface temperature by LES at heat flux of 721 kW/m<sup>2</sup>.

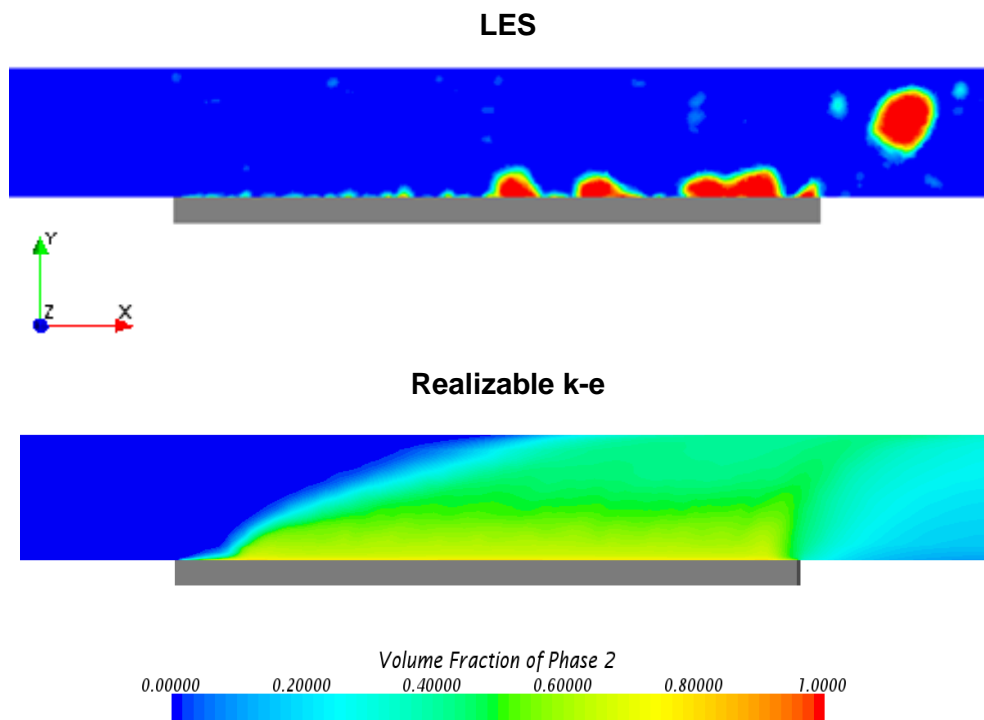
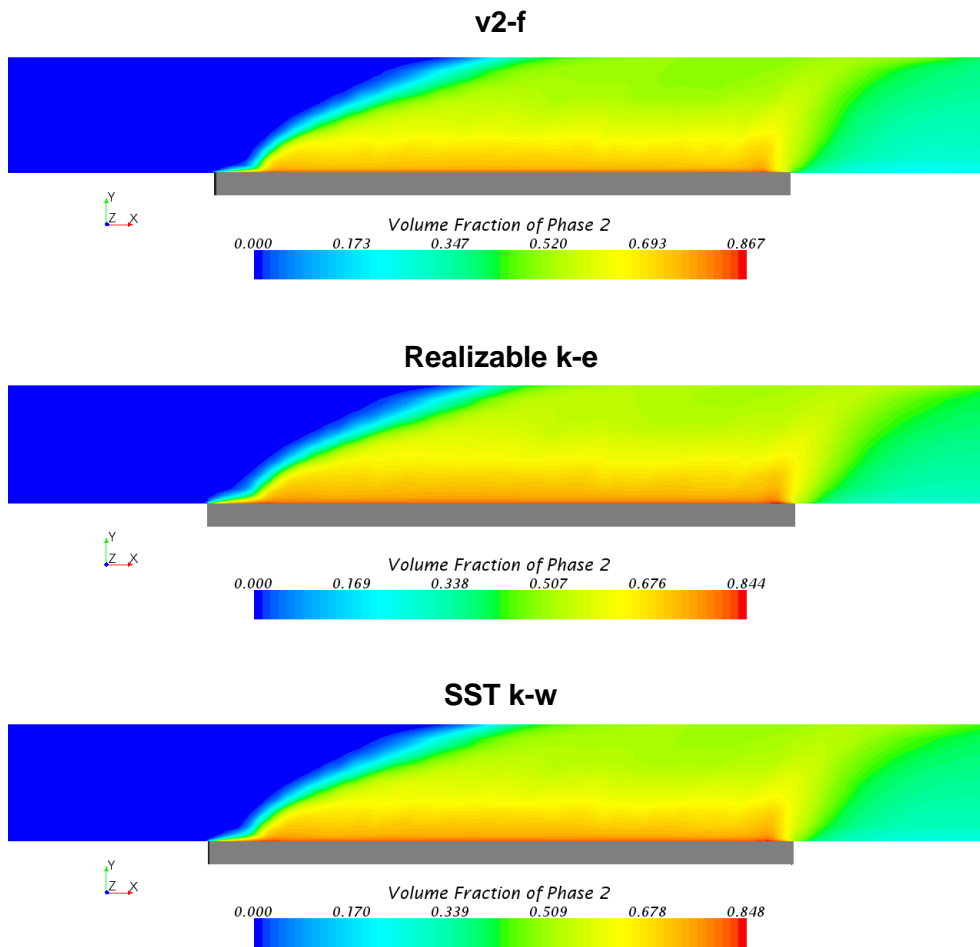
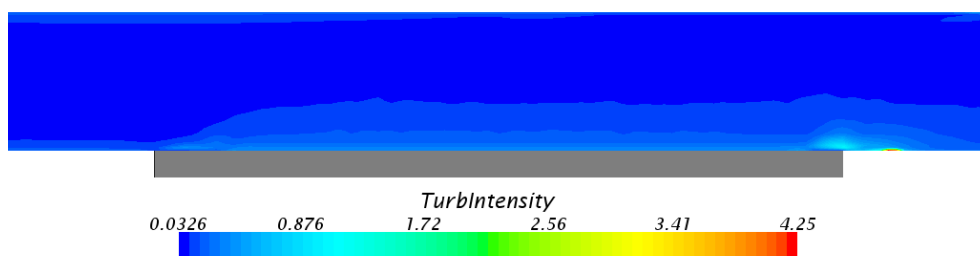


Figure 6. Predicted vapour volume fraction at heat flux of 721 kW/m<sup>2</sup>.



**Figure 7. Predicted vapour volume fractions by different turbulence models at heat flux of 1300 kW/m<sup>2</sup>.**



**Figure 8. Predicted turbulent intensity by realizable k-e turbulence model at heat flux of 721 kW/m<sup>2</sup>.**